2.3.3 State-Space Model for Unsteady Attached Flow

All other aerodynamic force terms in equations (2.10-2.13), can be calculated in the way shown in the previous section. The indicial responses for the remaining terms, taken from reference [5], are given by

$$\phi_q^I = exp\left(\frac{-t}{K_q T_I}\right) \tag{2.31}$$

$$\phi_q^C = \phi_\alpha^C = 1 - A_1 exp\left(-b_1\beta^2\frac{2V}{c}t\right) - A_2 exp\left(-b_2\beta^2\frac{2V}{c}t\right) \tag{2.32}$$

$$\phi_{\alpha M}^I = A_3 exp\left(\frac{-t}{b_3 K_{\alpha M} T_I}\right) + A_4 exp\left(\frac{-t}{b_4 K_{\alpha M} T_I}\right) \tag{2.33}$$

$$\phi_{qM}^I = exp\left(\frac{-t}{K_{qM} T_I}\right) \tag{2.34}$$

$$\phi_{qM}^C = 1 - A_5 exp\left(-b_5\beta^2\frac{2V}{c}t\right) \tag{2.35}$$

The total aerodynamic normal force and pitching moment under unsteady attached flow is the sum of the circulatory and noncirculatory responses due to changes in angle of incidence and pitch rate. For an aerofoil in continuous motion, these aerodynamic force components are found from the solution of the state-space ODEs of the form

$$\mathbf{x}' = \frac{c}{2V}\left(\mathbf{A}\mathbf{x} + \mathbf{B}\begin{Bmatrix}\alpha(S)\\ q(S)\end{Bmatrix}\right) \tag{2.36}$$

$$\begin{Bmatrix}C_N^P(S)\\ C_M^P(S)\end{Bmatrix} = \mathbf{C}\mathbf{x} + \mathbf{D}\begin{Bmatrix}\alpha(S)\\ q(S)\end{Bmatrix} \tag{2.37}$$

Note that in equation (2.36), the derivative is with respect to a nondimensional time S, where $S = \frac{2V}{c}t$. This is introduced here because the dynamic stall model which will be eventually written in nondimensional form. Earlier derivations in section 2.3.2 are performed in the physical time domain because of the way the indicial responses are defined.

The state-space constant matrices in equations (2.36) and (2.37) are given by

$$\mathbf{A} = \begin{bmatrix} a_{11} & 0 & 0 & 0 & 0 & 0 & 0 & 0 \\ 0 & a_{22} & 0 & 0 & 0 & 0 & 0 & 0 \\ 0 & 0 & a_{33} & 0 & 0 & 0 & 0 & 0 \\ 0 & 0 & 0 & a_{44} & 0 & 0 & 0 & 0 \\ 0 & 0 & 0 & 0 & a_{55} & 0 & 0 & 0 \\ 0 & 0 & 0 & 0 & 0 & a_{66} & 0 & 0 \\ 0 & 0 & 0 & 0 & 0 & 0 & a_{77} & 0 \\ 0 & 0 & 0 & 0 & 0 & 0 & 0 & a_{88} \end{bmatrix}, \mathbf{B} = \begin{bmatrix} 1 & 0.5 \\ 1 & 0.5 \\ 1 & 0 \\ 0 & 1 \\ 1 & 0 \\ 1 & 0 \\ 0 & 1 \\ 0 & 1 \end{bmatrix}$$

$$\mathbf{C} = \begin{bmatrix} c_{11} & c_{12} & c_{13} & c_{14} & 0 & 0 & 0 & 0 \\ c_{21} & c_{22} & 0 & 0 & c_{25} & c_{26} & c_{27} & c_{28} \end{bmatrix}, \mathbf{D} = \begin{bmatrix} \frac{4}{M} & \frac{1}{M} \\ -\frac{1}{M} & -\frac{7}{12M} \end{bmatrix}$$

where the elements in matrix $\mathbf{A}$ are given by

$$\begin{aligned} a_{11} &= -\frac{2V}{c} b_1 \beta^2, & a_{22} &= -\frac{2V}{c} b_2 \beta^2, \\ a_{33} &= -\frac{1}{K_\alpha T_I}, & a_{44} &= -\frac{1}{K_q T_I}, \\ a_{55} &= -\frac{1}{b_3 K_{\alpha M} T_I}, & a_{66} &= -\frac{1}{b_4 K_{\alpha M} T_I}, \\ a_{77} &= -\frac{2V}{c} b_5 \beta^2, & a_{88} &= -\frac{1}{K_{qM} T_I}, \end{aligned} \tag{2.38}$$

The elements in matrix $\mathbf{C}$ are given by

$$\begin{aligned} c_{11} &= C^S_{N\alpha} \frac{2V}{c} \beta^2 A_1 b_1, & c_{12} &= C^S_{N\alpha} \frac{2V}{c} \beta^2 A_2 b_2, \\ c_{13} &= \frac{4}{M} \left(\frac{-1}{K_{\alpha T_I}} \right), & c_{14} &= \frac{1}{M} \left(\frac{-1}{K_{q T_I}} \right), \\ c_{21} &= c_{11} \left(0.25 - x_{ac} \right), & c_{22} &= c_{12} \left(0.25 - x_{ac} \right), \\ c_{25} &= \frac{-1}{M} \left(\frac{-A_3}{b_3 K_{\alpha M} T_I} \right), & c_{26} &= \frac{-1}{M} \left(\frac{-A_4}{b_4 K_{\alpha M} T_I} \right), \\ c_{27} &= -\frac{C^S_{N\alpha}}{16} b_5 \beta^2 \left(\frac{2V}{c} \right), & c_{28} &= \frac{-7}{12M} \left(\frac{-1}{K_{qM} T_I} \right). \end{aligned} \tag{2.39}$$

and x_{ac} is the nondimensional position of the aerofoil aerodynamic centre.

The time constants used in expressions above are given by

$$K_q = \frac{0.75}{(1-M)+2\pi\beta^2 M^2(A_1b_1+A_2b_2)} \tag{2.40}$$

$$K_{\alpha M} = \left[\frac{A_3b_4+A_4b_3}{b_3b_4(1-M)}\right] \tag{2.41}$$

$$K_{qM} = \frac{7}{15(1-M)+3\pi\beta M^2 b_5} \tag{2.42}$$

where the parameters A_3, A_4, A_5, b_3, b_4, and b_5 are given in Table 2.3.1.

Finally, the circulatory and noncirculatory parts of the aerodynamic forces will be used separately in latter parts of the LB model. Hence, it is useful to define individual parts of these forces, and they are given by

$$C_N^C(S) = C_{N\alpha}^S \beta^2 \frac{2V}{c}\left(A_1b_1x_1+A_2b_2x_2\right) \tag{2.43}$$

$$C_N^I(S) = \frac{4}{M}\left(\frac{-1}{K_{\alpha T_I}}x_3+\alpha(S)\right)+\frac{1}{M}\left(\frac{-1}{K_{qT_I}}x_4+q(S)\right) \tag{2.44}$$

$$C_M^C(S) = (0.25-x_{ac})\,C_N^C(S)+\frac{C_{N\alpha}^S}{16}\left(A_5b_5\beta^2\frac{2V}{c}x_7\right) \tag{2.45}$$

$$\begin{aligned} C_M^I(S) = {} & \frac{-1}{M}\left(-\frac{A_3}{b_3K_{\alpha M}T_I}x_5-\frac{A_4}{b_4K_{\alpha M}T_I}x_6+\alpha(S)\right) \\ & -\frac{7}{12M}\left(\frac{-1}{K_{qM}T_I}x_8+q(S)\right) \end{aligned} \tag{2.46}$$

In summary, the total aerodynamic normal force C_N^P, and pitching moment C_M^P under unsteady attached flow can be found from the time histories of aerofoil motion $\alpha(S)$ and $q(S)$, and the state variables x_1-x_8, which are the solutions of the system of linear ODEs (2.36).

2.4 Trailing Edge Separated Flow

The first nonlinear part of the LB model is the simulation of trailing edge separation. Progressive trailing edge separation is usually present when the angle of incidence is near or greater than the static stall angle. Due to high adverse pressure gradients on the upper surface at high angle of incidence, the flow detaches from the surface to produce a turbulent wake. This causes a loss of circulation which introduces a non-linear force and moment.

The Kirchhoff theory introduced in section 2.2 forms the basis for modelling nonlinear aerodynamic forces under trailing edge separation. Three new state variables are introduced here: the normal force[3] $x_9 = C_N^*$, the dynamic trailing edge separation point $x_{10} = f^{**}$, and the dynamic trailing edge separation point $x_{12} = f_M$. Note that the numbering of these states is consistent with the original numbering presented in Reference [44]. The variable x_{11} will be used later in section 2.5 to model the effects of leading edge vortex shedding. The significance and derivation of these three new state variables will be explained later.

For the static case, the aerodynamic forces predicted by the Kirchhoff theory are given by equations (2.7-2.9). The equivalent dynamic equations are given by

$$C_N^f(S) = C_N^C(S)\left(\frac{1+\sqrt{x_{10}}}{2}\right)^2 \tag{2.47}$$

$$C_M^f(S) = \left[K_0 + K_1(1-\hat{x}) + K_2 sin(\pi\hat{x}^m)\right]C_N^C\left(\frac{1+\sqrt{\hat{x}}}{2}\right)^2 \tag{2.48}$$

$$C_C^f(S) = \eta C_{N\alpha}^S\left(\frac{C_N^C(S)}{C_{N\alpha}^S}\right)^2\sqrt{x_{10}} \tag{2.49}$$

where, in equation (2.48),

$$\hat{x} = \begin{cases} x_{10} & \text{if } x_{10} > x_{12} \\ x_{12} & \text{if } x_{10} \le x_{12} \end{cases} \tag{2.50}$$

From these expressions, it is apparent that in order to calculate aerodynamic loads of a moving aerofoil with trailing edge separated flow, it is important to first produce an accurate dynamic separation point f^{**}. For the static case, the normal force and pitching moment are functions of the trailing edge separation point f which is in turn a function of the angle

[3] In Leishman [44], this term is referred to as C_N'. It has been renamed to C_N^* here to avoid confusion with the derivatives with respect to S. Similarly, the terms f' and f'' in the same reference have also been renamed to f^* and f^{**}, respectively.

of incidence. However, for the dynamic case, due to the aerofoil pressure distribution and the unsteady boundary layer response, the movement of separation point slightly lags behind the corresponding instantaneous angle of incidence. Each cause of the delay will be investigated and modeled individually.

Leishman [44] suggests that there is a lag in the aerofoil leading edge pressure distribution with respect to normal force $C_N^P(S)$. The leading edge pressure plays a very important part in determining the onset of dynamic stall which will be discussed further in section 2.5. For the current application, the leading edge pressure lag can be simply modeled by applying a first order lag with a time delay constant T_P to $C_N^P(S)$ to produce a value $x_9 = C_N^*$. The lag equation is written as

$$x_9' = \frac{C_N^P - x_9}{T_P} \tag{2.51}$$

The time constant T_P is Mach number dependent and is given in Table 2.1. This value of delayed normal force is then used to produce an *equivalent* angle of incidence $\frac{x_9}{C_{N\alpha}^S}$. This angle of incidence is different from and should not be confused with the *effective* angle of incidence of a 2-DOF aerofoil which will be defined in chapter 3. The corresponding separation point $f^* = f\left(\frac{x_9}{C_{N\alpha}^S}, \alpha_1\right)$ is given as a function of the the equivalent angle of incidence, where f is given by equation (2.6).

The effects of unsteady boundary layer response can be modeled by the application of a first order lag to the value of f^*, with a time delay constant T_{f0}, to produce the final value of dynamic separation point $x_{10} = f^{**}$. The dynamic separation point is only used in calculation of normal force and chord force under separated flow. The pitching moment term is calculated using another variable $x_{12} = f_M$. This is because test results conducted by Leishman [6] have shown that the dynamic separation point fails to accurately predict the pitching moment during flow reattachment from deep stall regime. Hence, a separation point is proposed for use during this period with half the value of the time constant used in calculation of f^{**}. The states x_{10} and x_{12} are the solutions of the ODEs

$$x'_{10} = \frac{f\left(\frac{x_9}{C_{N\alpha}}, \alpha_1\right) - x_{10}}{T_f} \tag{2.52}$$

$$x'_{12} = \frac{f(\alpha, \alpha_1) - x_{12}}{0.50 T_{f0}} \tag{2.53}$$

The parameter T_f in equation (2.52) determines the amount of delay of x_{10} with respect to $f(\frac{x_9}{C_{N\alpha}}, \alpha_1)$. It effectively controls the velocity of the trailing edge flow separation point. Leishman [6] suggests that this speed is not constant, and that its value depends on the instantaneous flow conditions. Similarly, α_1 has been described as the static stall angle, but it is also used in the calculation as the reattachment angle. It is also argued that reattachment actually occurs at a lower angle than the separation, thus making α_1 another variable parameter.

The variations of parameters T_f and α_1 are explained in the following subsections. The values of T_{f0} and α_{10} are given in Table 2.1.

Vortex shedding phase ($|x_9| \geq C_{N1}$) This phase occurs when the leading edge pressure reaches a critical value. Since the leading edge pressure relates directly to the normal force, it is possible, and also more convenient, to make calculations using the normal force. C_{N1} is defined as the critical normal force, which corresponds to the critical leading edge pressure. The effects of vortex shedding will be explored in more detail in section 2.5.

If $|x_9| = C_{N1}$ and $|x_9|$ is increasing, a vortex is shed from the leading edge and the vortex time, τ_v, starts ($\tau_v = 0$). The vortex time τ_v progresses at the same rate as the nondimensional time S. The parameter T_{vl} is defined as the time the vortex takes to travel one chord length, i.e. when $\tau_v = T_{vl}$, the vortex is positioned over the aerofoil trailing edge.

During the vortex shedding phase the variation of parameter T_f is given in Table 2.3.

	$0 \leq \tau_v \leq T_{vl}$	$T_{vl} < \tau_v \leq 2T_{vl}$	$2T_{vl} < \tau_v$
$\alpha\alpha' \geq 0$	$T_f = T_{f0}$	$T_f = \frac{1}{3}T_{f0}$	$T_f = 4T_{f0}$
$\alpha\alpha' < 0$	$T_f = \frac{1}{2}T_{f0}$	$T_f = \frac{1}{2}T_{f0}$	$T_f = 4T_{f0}$

Table 2.3: Variations of parameters during vortex shedding phase

The parameter α_1 does not depend on τ_v, and it is given by

$$\alpha_1 = \begin{cases} \alpha_{10} & \text{if } \alpha\alpha' \geq 0 \\ \alpha_{10} - (1 - x_{10})^{0.25}\delta_{\alpha_1} & \text{if } \alpha\alpha' < 0 \end{cases} \tag{2.54}$$

where δ_{α_1} is a user-defined parameter and it is given as a function of M in Table 2.1.

Flow reattachment phase ($|x_9| < C_{N1}$) This phase begins when $|x_9| = C_{N1}$ and $|x_9|$ is decreasing. This is taken into account by choosing

$$T_f = \begin{cases} T_{f0} & \text{if } x_{10} \geq 0.7 \\ \frac{1}{2}T_{f0} & \text{if } x_{10} < 0.7 \end{cases} \tag{2.55}$$

$$\alpha_1 = \alpha_{10} \tag{2.56}$$

2.5 Dynamic Stall (Vortex Induced Airloads)

The final part of the dynamic stall model corresponds to the vortex induced airloads. Leishman and Beddoes [8] state that the accurate prediction of onset of leading edge separation is very important in modeling dynamic stall. They suggest that flow separation occurs when a critical leading edge pressure and pressure gradient are reached. They also state that the leading edge pressures are related to normal force. This leads to a very simple criteria for leading edge separation, as separation occurs when the delayed normal force exceeds the critical value, i.e. $C_N^* \geq C_{N1}$, where C_{N1} is the critical normal force. The value of C_{N1} varies with Mach number and is depicted in figure 2.8 for the aerofoil NACA0012.

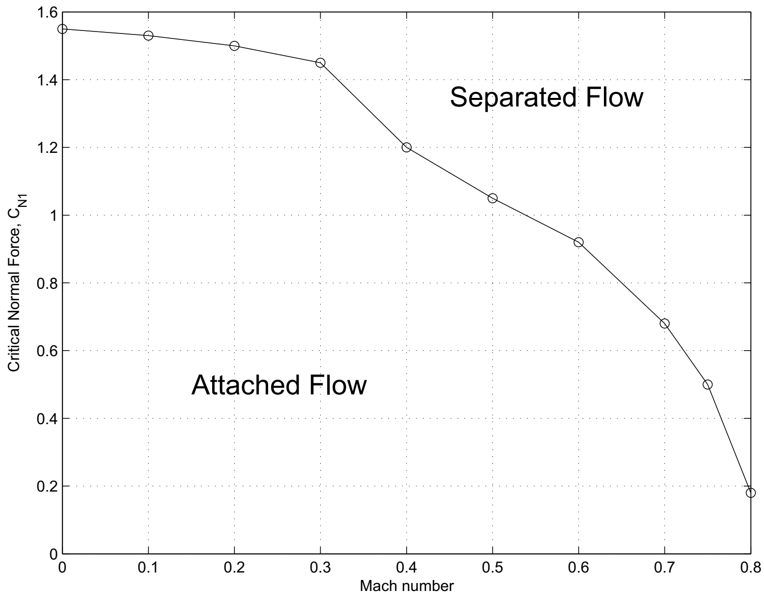

Figure 2.8: Critical normal force separation onset boundary for aerofoil NACA0012 adopted from reference [6].

Here the normal force and pitching moment generated by the presence of vortex are given by

$$C_N^v = x_{11} \tag{2.57}$$

$$C_M^v = \begin{cases} -0.25\left(1 - cos\left(\frac{\pi\tau_v}{T_{vl}}\right)\right)x_{11} & \text{if } \tau_v \leq 2T_{vl} \\ 0 & \text{if } \tau_v > 2T_{vl} \end{cases} \tag{2.58}$$

The state x_{11} is the solution of

$$x'_{11} = \begin{cases} c'_v - \frac{x_{11}}{T_v} & \text{if } \alpha c'_v \geq 0 \text{ and } 0 < \tau_v < 2T_{vl} \\ -\frac{x_{11}}{T_v} & \text{otherwise} \end{cases} \tag{2.59}$$

The vortex feed, c_v, determines the strength of vortex induced normal force and is defined as the instantaneous excess normal force, $c_v = C_N^C - C_N^f$. A negative vortex feed is not allowed, therefore equation (2.59) has two forms, depending on the direction of the vortex feed as determined by the sign of the term $\alpha c_v'$ [69]. Its derivative, c_v', is given as

$$\begin{aligned} c_v' &= -C_{N\alpha}\left(\frac{2V}{c}\right)\beta^2\left(A_1 b_1 x_1 + A_2 b_2 x_2\right)\frac{x_{10}'}{4}\left(1+\frac{1}{\sqrt{x_{10}}}\right) \\ &\quad + C_{N\alpha}\frac{2V}{c}\beta^2\left[A_1 b_1 x_1' + A_2 b_2 x_2'\right]\left(1-\left(\frac{1+\sqrt{x_{10}}}{2}\right)^2\right) \end{aligned}$$

From equation (2.59), the rate of change of vortex induced normal force is controlled by the parameter T_v. This parameter is also subject to change according to the flow condition. Leishman [6] suggests that the vortex lift decays more rapidly after the vortex has been convected past the trailing edge, and this can be modeled by lowering the parameter T_v.

During the vortex shedding phase ($|x_9| \geq C_{N1}$), the parameter T_v is given in Table 2.4.

	$0 \leq \tau_v \leq T_{vl}$	$T_{vl} < \tau_v \leq 2T_{vl}$	$2T_{vl} < \tau_v$
$\alpha\alpha' \geq 0$	$T_v = T_{v0}$	$T_v = 0.25T_{v0}$	$T_v = 0.90T_{v0}$
$\alpha\alpha' < 0$	$T_v = 0.50T_{v0}$	$T_v = 0.50T_{v0}$	$T_v = 0.90T_{v0}$

Table 2.4: Variations of parameters during vortex shedding phase

Finally, the flow reattachment phase ($|x_9| < C_{N1}$) is characterised by $T_v = T_{v0}$.

2.6 Standard Formulation

This section describes the standard (indicial) formulation of the LB model. This section has been included here for the purpose of methodology verification. The comparison of aerodynamic forces predicted by the state-space and standard formulations will be shown in section 2.7.

The standard formulation of the LB model for an aerofoil proposed in reference [8] makes use of the recurrence algorithm developed by Beddoes [40] to calculate the cumulative indicial responses as opposed to the state-space method shown in previous sections. The approach is based on solution of the